AFRL-RD-PS-
TR-2014-0022
AFRL-RD-PS-
TR-2014-0022

ATOMIC LAYER DEPOSITION OF METAL OXIDES ON sp^2-GRAPHITIC CARBON SUBSTRATES

Steven M. George

University of Colorado
Dept. of Chemistry & Mechanical Engineering
215 UCB
Boulder, CO 80309-0215

31 March 2014

Final Report

AIR FORCE RESEARCH LABORATORY
Directed Energy Directorate
3550 Aberdeen Ave SE
AIR FORCE MATERIEL COMMAND
KIRTLAND AIR FORCE BASE, NM 87117-5776

NOTICE AND SIGNATURE PAGE

Using Government drawings, specifications, or other data included in this document for any purpose other than Government procurement does not in any way obligate the U.S. Government. The fact that the Government formulated or supplied the drawings, specifications, or other data does not license the holder or any other person or corporation; or convey any rights or permission to manufacture, use, or sell any patented invention that may relate to them.

This report was cleared for public release by the Air Force Research Laboratory RD Public Affairs Office and is available to the general public, including foreign nationals. Copies may be obtained from the Defense Technical Information Center (DTIC) (http://www.dtic.mil).

AFRL-RD-PS-TR-2014-0022 HAS BEEN REVIEWED AND IS APPROVED FOR PUBLICATION IN ACCORDANCE WITH ASSIGNED DISTRIBUTION STATEMENT.

SUSAN HEIDGER, DR-IV
Program Manager

STEPHEN T. MARTINICK, DR-IV
Chief, High Power Electromagnetics Division

This report is published in the interest of scientific and technical information exchange, and its publication does not constitute the Government's approval or disapproval of its ideas or findings.

REPORT DOCUMENTATION PAGE

Form Approved
OMB No. 0704-0188

1. REPORT DATE *(DD-MM-YYYY)*	**2. REPORT TYPE**	**3. DATES COVERED** *(From - To)*
31-03-2013	Final Report	28-08-2012 – 28-02-2014

4. TITLE AND SUBTITLE

Atomic Layer Deposition of Metal Oxides on sp²-Graphitic Carbon

5a. CONTRACT NUMBER
FA9451-12-1-0229

5b. GRANT NUMBER

5c. PROGRAM ELEMENT NUMBER
1620

6. AUTHOR(S)

Steven M. George

5d. PROJECT NUMBER

5e. TASK NUMBER
D050 HN

5f. WORK UNIT NUMBER
PPM00018659 CO

7. PERFORMING ORGANIZATION NAME(S) AND ADDRESS(ES)

University of Colorado
Depts. of Chemistry & Mechanical Engineering
Boulder, CO 80309

8. PERFORMING ORGANIZATION REPORT NUMBER

9. SPONSORING / MONITORING AGENCY NAME(S) AND ADDRESS(ES)

Air Force Research Laboratory
3550 Aberdeen Avenue SE
Kirtland AFB, NM 87117-5776

10. SPONSOR/MONITOR'S ACRONYM(S)
AFRL/RDHP

11. SPONSOR/MONITOR'S REPORT NUMBER(S)
AFRL-RD-PS-TR-2014-0022

12. DISTRIBUTION / AVAILABILITY STATEMENT
Approved for public release; distribution unlimited.

13. SUPPLEMENTARY NOTES
PA# 377ABW-2014-0671 Government Purpose Rights

14. ABSTRACT

This research concentrated on the growth and characterization of metal oxide ALD films on sp2-graphitic carbon substrates. Metal oxide ALD films on sp2-graphitic carbon were also evaluated for their ability to serve as electrodes for Li ion batteries and for pseudocapacitance supercapacitors. The research explored the ALD nucleation procedure based on NO2 and TMA. Al2O3 ALD films resulting from the nucleation procedure were analyzed using electrochemical methods with cyclic voltammetry and electrochemical impedance spectroscopy (EIS). Other metal oxide ALD films such as TiO2 and ZnO were used for electrodes for Li ion batteries and pseudocapacitance supercapacitors.

15. SUBJECT TERMS
F-16 Aircraft, High Power Microwave (HPM), High Power RD (HPRF), Electromagnetic Interference (EMI), Electromagnetic Hardening, Aircraft Electromagnetic Effects, Transfer Function

16. SECURITY CLASSIFICATION OF:			**17. LIMITATION OF ABSTRACT**	**18.NUMBER OF PAGES**	**19a. NAME OF RESPONSIBLE PERSON**
					Susan Heidger
a. REPORT	**b. ABSTRACT**	**c. THIS PAGE**	SAR	26	**19b. TELEPHONE NUMBER** *(include area code)*
UNCLASSIFIED	UNCLASSIFIED	UNCLASSIFIED			505-853-4707

Standard Form 298 (Rev. 8-98)
Prescribed by ANSI Std. 239.18

This page intentionally left blank.

TABLE OF CONTENTS

LIST OF FIGURES

Page

1.0 SUMMARY

This research concentrated on the growth and characterization of metal oxide atomic layer deposition (ALD) films on sp^2-graphitic carbon substrates. Metal oxide ALD films on sp^2-graphitic carbon were also evaluated for their ability to serve as electrodes for Li ion batteries and for pseudocapacitance supercapacitors. The research explored the ALD nucleation procedure on sp_2-graphitic carbon based on NO_2 and TMA. Al_2O_3 ALD films resulting from the nucleation procedure were analyzed using electrochemical methods with cyclic voltammetry and electrochemical impedance spectroscopy (EIS). Other metal oxide ALD films, such as TiO_2 ALD and ZnO ALD, were explored for electrochemical application in Li ion batteries and pseudocapacitance supercapacitors.

2.0 INTRODUCTION

The nucleation and growth of thin metal oxides on sp^2 carbon surfaces including graphene, carbon nanotubes, and other Buckminster fullerenes has wide implications for semiconductor manufacturing[1–3], electrochemical energy conversion[4], batteries[5–8], and supercapacitors.[9–11] The electrical conductivity of the sp^2 carbon support is vital in these applications, signaling the necessity of a non-covalent nucleation chemistry to act as an anchor for successive ALD chemistry.

A wide variety of non-covalent chemistries have been explored for nucleation on sp^2 carbon surfaces.[12] Of these, none is so widely used as NO_2/TMA pretreatment.[2,3,11,13–15] The NO_2/TMA chemistry was originally developed by Roy Gordon's research group at Harvard, and was performed at 25°C.[16] Successive work by our group showed the viable use of a NO_2/TMA pretreatment temperature as high as 180°C, but with apparent CVD-like deposition.[17] In this work, we study the use of the NO_2/TMA pretreatment procedure at 150°C and its effects on the resulting film thickness and quality.

This work experimentally evaluated the impact of the nitrogen dioxide and trimethylaluminum (NO_2/TMA) pretreatment on the subsequent nucleation and growth of atomic layer deposition aluminum oxide (Al_2O_3) on a model sp^2 carbon substrate. Trimethylaluminum (TMA) and water (H_2O) were used to grow Al_2O_3 on exfoliated highly ordered pyrolitic graphite (HOPG) at 150˚C˚with and without pretreatment of 5 cycles of NO_2/TMA. The ALD films on HOPG samples were evaluated using spectroscopic ellipsometry and electrochemical analysis to

determine film thickness and quality. We found that 5 cycles of NO_2/TMA deposits a ~8 Å thick film on HOPG. The NO_2/TMA pretreatment enabled the nucleation of a high quality, conformal, continuous ALD film after as few as 20 ALD cycles of TMA/H_2O. With no NO_2/TMA pretreatment, 100 ALD cycles of TMA/H_2O were necessary to produce a continuous film. Films grown following NO_2/TMA pretreatment were also demonstrated to have better stability in an aqueous environment.

In addition to the study of the nucleation treatment based on nitrogen dioxide and trimethylaluminum (NO_2/TMA), various metal oxide ALD films were grown on graphene and carbon nanotube substrates. These metal oxide ALD films were chosen because of their electrochemical relevance to serve as electrodes for Li ion batteries and pseudocapacitance supercapacitors. This work was performed in collaboration with Prof. Jie Lian at Rensselaer Polytechnic Institute (RPI). Graphene and carbon nanotube substrates are ideal electrode supports because of their high surface area and high electrical conductivity. We obtained very favorable results using TiO_2 ALD and ZnO ALD. The papers published or in press from this collaboration are in the Appendix.

3.0 METHODS, ASSUMPTIONS AND PROCEDURES

3.1 Sample Preparation

A model sp^2 carbon surface was obtained by exfoliating highly ordered pyrolitic graphite (HOPG) (SPI supplies SPI-2 Grade 20x20x1mm) onto conductive copper tape (3M single sided Cu conductive tape, 1” width). Some photographs illustrating this procedure are shown in Figure 1. Photographs of the procedure include (1) applying copper tape to HOPG, (2) exfoliating HOPG film, (3) punching out a 5/8” diameter disc of HOPG on copper tape, and (4) the completed HOPG substrate. After ALD growth on these samples, the 5/8” disc was used for electrochemical evaluation. Silicon pieces with a native oxide (Si) with dimensions of 1”x1” were cut from 6” silicon wafers (Silicon Valley Microelectronics), rinsed with acetone (Fisher, Certified ACS), and methanol (EMD Millipore HPLC grade), dried using UHP nitrogen (Airgas), and included in reactor runs. These silicon wafers served as reference samples to compare the deposition on the HOPG and silicon substrates.

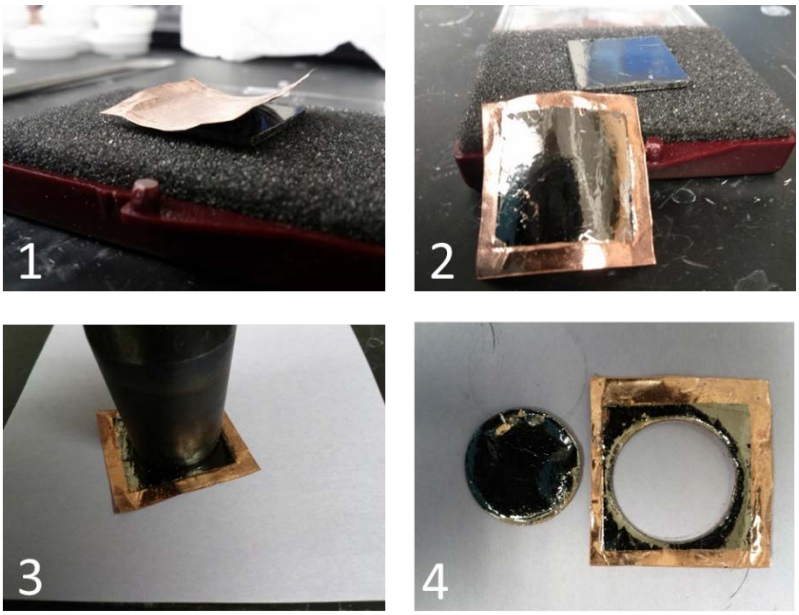

Figure 1. Photographs of Procedure used to Produce a Model sp^2 Carbon Surface Including (1) Applying Copper Tape to HOPG, (2) Exfoliating HOPG Film, (3) Punching Out a Disc of HOPG on Copper Tape, and (4) Completed HOPG Substrate

3.2 ALD Growth

Atomic layer deposition was carried out simultaneously on HOPG and Si samples in a custom viscous-flow reactor at 150˚C˚and ~1 Torr under continuous argon purge (Airgas Prepurified).[22] Aluminum oxide was grown using sequential exposures of (A) trimethylaluminum (TMA) (Aldrich 97%) and (B) water (H_2O) (B&J Brand® HPLC Grade). Peak dose pressures for both precursors were tuned to ~200mTorr above base pressure, with a timing sequence for A:Purge:B:Purge ALD cycles of 0.5s:45s:0.5s:45s. Nucleation chemistry was carried out using (C) nitrogen dioxide (NO_2) (Aldrich 99.5) and (A) TMA in a timing sequence for C:Purge:A:Purge nucleation cycles of 0.2s:45s:0.5s:45s.

3.3 Sample Characterization

3.3.1 X-ray Reflectivity

The thickness and density of the ALD coatings on Si were evaluated using X-ray reflectivity (XRR). XRR measurements were performed using a Bede D-1 Diffractometer. X-ray radiation with a wavelength of 1.54Å was used for measurements, corresponding to the Cu-Kα transition. Film thicknesses and densities were modeled using Bede REFS.

3.3.2 Spectroscopic Ellipsometry

The thickness, roughness, and void volume of ALD films on HOPG samples were evaluated using spectroscopic ellipsometry (SE). SE measurements were performed using a M-2000 spectroscopic ellipsometer (J.A. Woollam Co., Inc.). Film properties were modeled using CompleteEASE v.4.55 (J.A. Woollam Co., Inc.) with a Kramers-Kronig consistent B-spline model for the HOPG substrate, and a Cauchy model for the ALD films. ALD film thicknesses on Si were also determined by SE and benchmarked against XRR measurements on Si samples.

3.3.3 Electrochemical Evaluation

The porosity of insulating films on conducting substrates can be evaluated by determining the charge-transfer resistance at the open-circuit potential.[18–20] To determine charge-transfer resistances, Electrochemical Impedance Spectroscopy (EIS) and Linear Sweep Voltammetry (LSV) were performed on ALD-coated HOPG samples using a 2-channel SP-300 Potentiostat with Low Current Probes (BioLogic). EIS measurements were performed from 3MHz to 10mHz using multi-sine measurements for low frequencies, and EIS data was fit using Biologic's EC-Lab software. Linear sweep voltammetry was performed at a sweep rate of 1mV/s in a 200mV window surrounding the open-circuit potential, and the slope of the I-V curve at zero current was used to determine the charge transfer resistance.

These electrochemical measurements were performed in custom electrochemical cells. Evaluation was conducted in 0.10 M sodium sulfate (Alfa Aesar, 99.99% metals basis) aqueous electrolyte under a continuous argon (Airgas, Prepurified) purge. Platinum counter electrodes and saturated Ag/AgCl reference electrodes (BASi) were used for these measurements.

4.0 RESULTS AND DISCUSSION

4.1 Growth on HOPG

Figure 2 shows the modeled SE thickness and void volume using the effective medium approximation (EMA) after 20-200 ALD cycles of TMA/H_2O with and without NO_2/TMA pretreatment. The growth rate on Si was 1.3Å/cycle and on HOPG was 1.4Å/cycle. These growth rates agree with previously reported values of ~1.2 Å/cycle at 150°C.[21,22]

The top of Figure 2 shows that 5 cycles of NO_2/TMA pretreatment result in a thickness increase of ~8.2Å on the HOPG samples. In contrast, no thickness increase is observed from pretreatment with 5 cycles of NO_2/TMA on Si samples as shown in the inset. This indicates that the NO_2/TMA pretreatment deposits a nucleation layer on HOPG, but not on Si. Furthermore, the void space is observed to be lower for all ALD Al_2O_3 film thicknesses on HOPG when using the NO_2/TMA pretreatment. This indicates that a higher-quality ALD film is obtained on HOPG with the NO_2/TMA pretreatment.

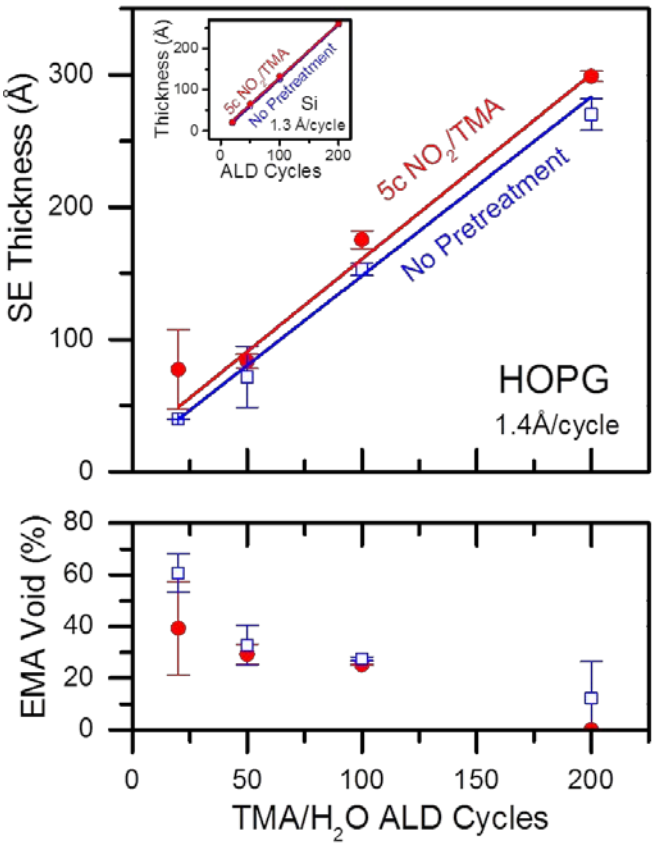

Figure 2. Spectroscopic Ellipsometry Model Results for Thickness (top) and Void Volume (bottom) vs TMA/H_2O ALD Cycles on HOPG Substrates with no Pretreatment (blue) and 5 Cycles of NO_2/TMA Pretreatment (red). The Inset in the Top Section Shows the XRR Thickness vs ALD Cycles for Growth on Si

4.2 Electrochemical Evaluation

Figure 3a shows the model circuit used to fit EIS data, where "R" indicates a resistor and "Q" indicates a constant phase element. Figure 3b shows measured EIS spectra and model fits for HOPG samples with 0-200 cycles TMA/H_2O without NO_2/TMA pretreatment. In this Nyquist plot, the radius of the semi-circle is indicative of the charge-transfer resistance for the electrode/electrolyte interface. A smaller radius indicates a lower charge-transfer resistance. Here, we note that after 20 and 50 ALD cycles; the measured charge-transfer resistances are *lower* than the uncoated HOPG substrate, while after 100 and 200 ALD cycles, the charge-transfer resistance is significantly larger than the uncoated HOPG substrate.

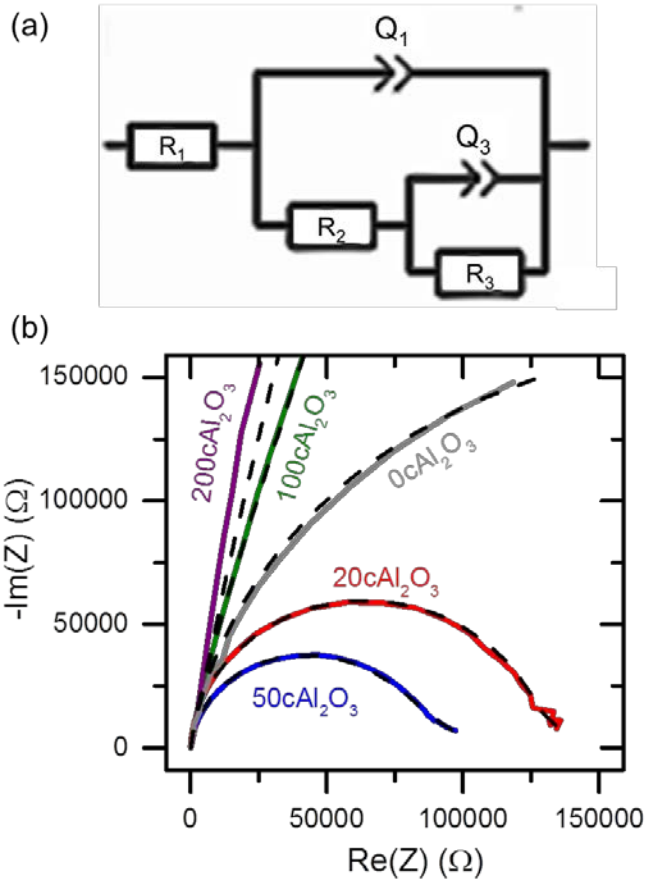

Figure 3. Electrochemical Impedance Spectroscopy Model Circuit (a) used to Fit Nyquist Plot of Measured Data (b) for Al_2O_3 ALD on HOPG Substrates with No Pretreatment. Dashed Lines in (b) are Model Fits

The total charge-transfer resistances from LSV and EIS are shown for TMA/H_2O on HOPG with no nucleation in Figure 4a. With no NO_2/TMA pretreatment, the TMA/H_2O chemistry is expected to nucleate at step-edges and defect sites on the HOPG surface. After enough ALD cycles, the ALD film will coalesce into a continuous film as shown in the inset graphic. Theoretically, charge-transfer resistances as measured by LSV and EIS should agree. The resistance values measured by LSV and EIS do agree closely for most conditions. The differences between resistance values measured by LSV and EIS arise from the wider potential window used to calculate the resistance in the LSV measurements, and from modeling limitations for EIS measurements. Any non-linearity in the LSV curve at zero current will result in an artificially lower modelled charge-transfer resistance. Furthermore, the charge-transfer resistances as measured by EIS are limited by the EIS model and curve-fitting, which were observed to be less accurate for very high charge transfer resistances.

In Figure 4a, the dramatic increase in charge-transfer resistance at >100 ALD cycles indicates that the ALD film has coalesced and is preventing the electrolyte from contacting the bare HOPG. The low resistances with 20 and 50 ALD cycles leave one to question how the presence of small amounts of Al_2O_3 at step edges and defect sites would lead to a *decrease* in charge-transfer resistance. This phenomenon could be due to the hydrophilic Al_2O_3 enabling ions to adsorb closer to the electrode surface. The Al_2O_3 surface will be covered with Al-OH hydroxyl species. These Al-OH hydroxyl species will interact favorably with H_2O molecules. In addition, the Al-OH hydroxyl species also are known to accept H^+ ions from water at neutral pH values to become Al-OH_2^+. These Al-OH hydroxyl species may facilitate charge transfer at the interface between HOPG and water.

The charge-transfer resistances from LSV and EIS are shown for TMA/H_2O on HOPG with 5 cycles NO_2/TMA pretreatment in Figure 4b. With NO_2/TMA pretreatment, the TMA/H_2O chemistry is expected to grow uniformly on the HOPG surface and result in a continuous ALD film even after very few ALD cycles as shown in the inset graphic. The very high charge transfer resistances after only 20 cycles of TMA/H_2O verifies this expectation, and the charge transfer resistance remains very high for all ALD Al_2O_3 thicknesses.

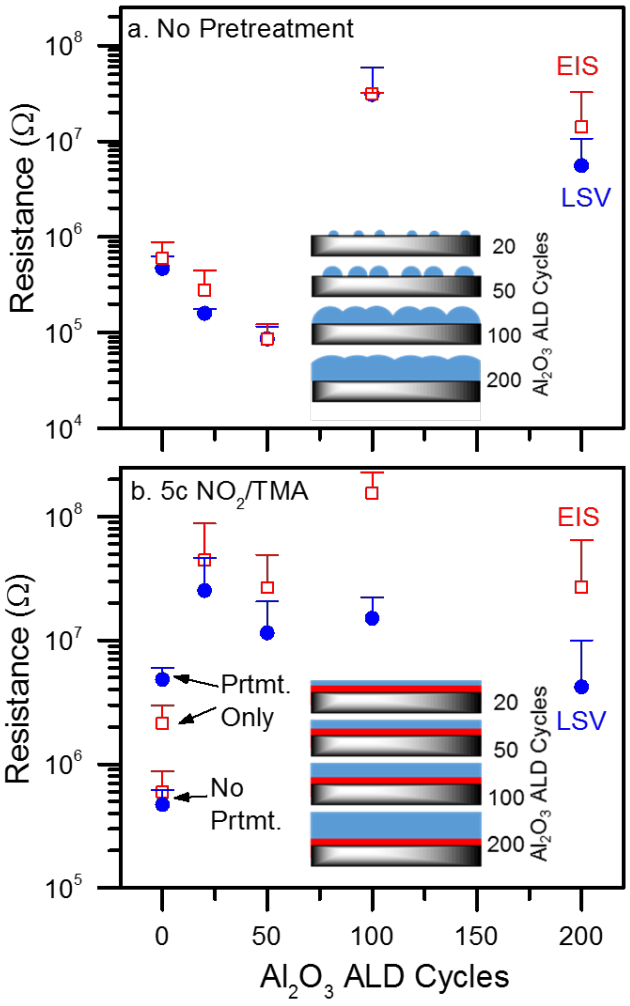

Figure 4. Charge-Transfer Resistance vs Number of Al_2O_3 ALD Cycles from Linear Sweep Voltammetry and Electrochemical Impedance Spectroscopy Measurements for Al_2O_3 Films on HOPG with (a) No Pretreatment, and (b) 5 Cycles of NO_2/TMA Pretreatment

4.3 Porosity Calculations

The total charge-transfer resistances from LSV and EIS were used to estimate the through-film porosity of the ALD coatings according to $P \cong \frac{R_{bare}}{R_{coated}}$.[18] P is the fractional through-film porosity of the coating, R_{bare} is the total charge-transfer resistance of the bare substrate, and R_{coated} is the total charge-transfer resistance of the coated substrate. The through-film porosities of ALD-coated Al_2O_3 with no pretreatment and with 5 cycles NO_2/TMA

pretreatment are shown in Figures 5a and 5b, respectively. These electrochemically-derived through-film porosities are distinct from the EMA void volume modeled above using spectroscopic ellipsometry and the two models cannot be compared one-to-one. The EMA void volume models the void space in the film, including surface roughness and isolated pockets of void space, whereas the through-film porosity only accounts for continuous pores traversing the entire thickness of the film from substrate to surface. With this in mind, EMA void volumes are expected to be greater than modeled through-film porosities from electrochemical measurements, which we do observe for most conditions.

In Figure 5a, the 20 and 50 cycles without pretreatment show a through-film porosity > 100% due to measured charge transfer resistances anomalously lower than the bare substrate as mentioned above. After 100 and 200 ALD cycles with no NO_2/TMA pretreatment, the through-film porosity is <10% In Figure 5b, the through-film porosity for all ALD Al_2O_3 thicknesses with 5 cycles of NO_2/TMA pretreatment are <10%, with EIS measurements indicating some through-film porosities of <1%. These results indicate that the NO_2/TMA pretreatment enables a much higher quality ALD film on the HOPG surface than is obtained with no NO_2/TMA pretreatment.

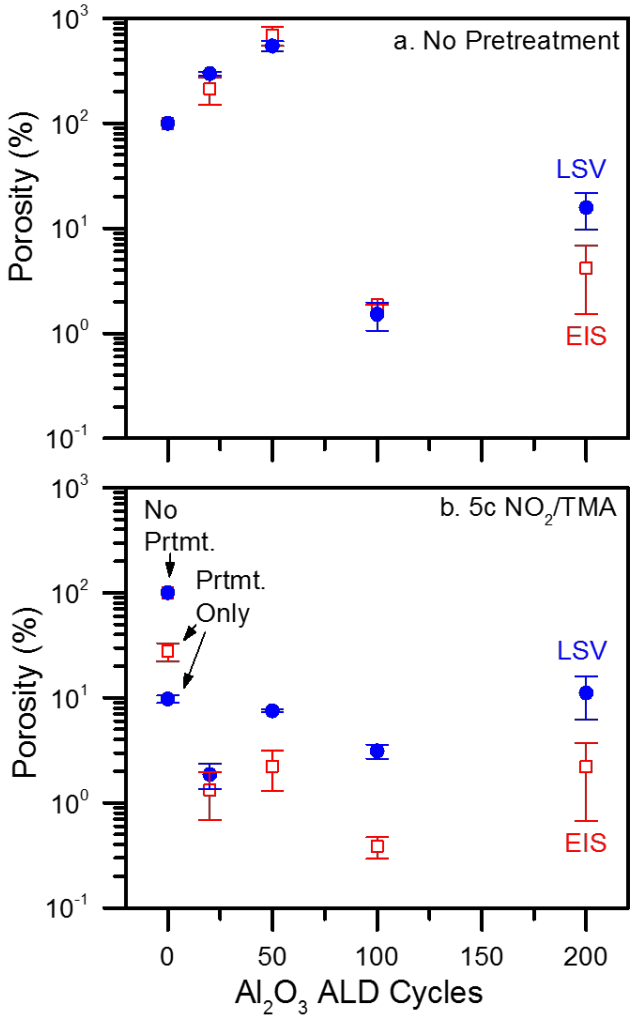

Figure 5. Calculated Porosity vs Number of Al_2O_3 ALD Cycles from Linear Sweep Voltammetry and Electrochemical Impedance Spectroscopy Measurements for Al_2O_3 Films on HOPG with (a) No Pretreatment, and (b) 5 Cycles of NO_2/TMA Pretreatment

Figure 6 shows the relative stability of ALD-Al_2O_3 films in 0.10 M aqueous sodium sulfate electrolyte with and without pretreatment. This data indicates that with 5 cycles of NO_2/TMA and only 50 cycles of TMA/H_2O, the initial porosity of ~3% does not increase until ~100hrs in an aqueous environment. This ~90Å thick film grown with NO_2/TMA pretreatment is more stable in an aqueous environment than a ~250 Å thick film grown with no pretreatment and 200 cycles of TMA/H_2O, which has an initial through-film porosity of ~4% that increases up to ~8% after only 50 hours. This data suggests that the initial quality of the ALD film has a

severe impact on the stability in an aqueous environment, and that by increasing the film quality with NO_2/TMA pretreatment, the stability in water is improved.

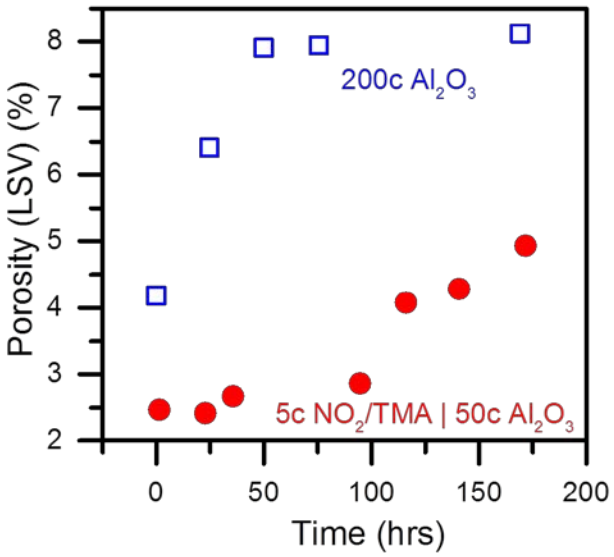

Figure 6. Porosity vs Time from Linear Sweep Voltammetry Measurements for HOPG Samples in 0.10M Na_2SO_4 Aqueous Electrolyte

4.4 Applications of ALD on sp^2 Graphitic Carbon Substrates

In addition to the study of the nucleation treatment based on nitrogen dioxide and trimethylaluminum (NO_2/TMA), various metal oxide ALD films were grown on graphene and carbon nanotube substrates. These metal oxide ALD films were chosen because of their relevance to serve as electrodes for Li ion batteries and pseudocapacitance supercapacitors. This work was performed in collaboration with Prof. Jie Lian at Rensselaer Polytechnic Institute (RPI). Graphene and carbon nanotube substrates are ideal electrode supports because of their high surface area and high electrical conductivity.

4.4.1 TiO_2 ALD as Anode Material for Li Ion Batteries

We obtained very favorable results using TiO_2 ALD anode material on high surface area graphene sheets for Li ion batteries. An Al_2O_3 ALD ultrathin layer was used as an adhesion layer for conformal deposition of the TiO_2 ALD films at 120°C onto the conducting graphene sheets. The TiO_2 ALD films on the Al_2O_3 ALD adhesion layer were nearly amorphous and

conformal to the graphene sheets. These nanoscale TiO_2 coatings minimized the effect of the low diffusion coefficient of lithium ions in bulk TiO_2. The TiO_2 ALD films exhibited stable capacities of ~120 mAh g^{-1}, and ~100 mAh g^{-1} at high cycling rates of 1 A g^{-1} and 2 A g^{-1}, respectively. The TiO_2 ALD films also displayed an excellent cycling stability with ~95% of the initial capacity remaining after 500 cycles. These results illustrate that ALD can provide a useful method to deposit electrode materials on high surface area substrates for Li ion batteries. The published results from this study are given in the Appendix.

4.4.2 TiO_2 ALD for Pseudocapacitance Supercapacitors

We obtained very favorable results using TiO_2 ALD on high surface area graphene (G) sheets and carbon nanotube (CNT) samples to fabricate pseudocapacitance supercapacitors. An ultrathin Al_2O_3 adhesion layer was employed to obtain a conformal TiO_2 ALD films. Using 1 M KOH as the electrolyte, the electrochemical characteristics of TiO_2 ALD films grown using 25 and 50 TiO_2 ALD cycles were then determined using cyclic voltammetry, galvanostatic charge/discharge curves and electrochemical impedance spectroscopy. Because the TiO_2 ALD films were ultrathin, the poor electrical conductivity and low ionic diffusivity of TiO_2 did not limit the ability of the TiO_2 ALD films to display high specific capacitance. The specific capacitances of the TiO_2 ALD-coated G and CNT samples after 50 TiO_2 ALD cycles were 97.5 F/g and 135 F/g, respectively, at 1 A/g. The pseudocapacitance of the TiO_2 ALD films greatly exceeded the electric double layer capacitance of the uncoated G and CNT samples.

The galvanostatic charge/discharge experiments also revealed that the charge storage was dependent on the thickness of the TiO_2 ALD film. This observation argues that the pseudocapacitance is derived largely from the TiO_2 bulk and is not limited to the TiO_2 surface. An optimized asymmetric cell was also developed based on TiO_2 ALD-coated CNT as the positive electrode and uncoated CNT as the negative electrode. This energy storage device could be reversibly operated over a wide voltage range of 0-1.5 V in the aqueous 1 M KOH electrolyte. An energy density of 4.47 Wh/kg was achieved on the basis of the total weight of both electrodes. The results of this study demonstrate that metal oxide ALD on high surface area conducting carbon substrates can be used to fabricate high energy storage supercapacitors. The published results from this study are also given in the Appendix.

4.4.3 ZnO ALD Quantum Dots on Graphene for Ultraviolet Sensing

As part of our work on ALD on grapheme, we also fabricated a composite material composed of ZnO ALD quantum dots on grapheme. The ZnO ALD quantum dots did not require an Al_2O_3 ALD adhesion layer. In contrast, the ZnO ALD quantum dots depend on the poor nucleation of ZnO ALD on grapheme. A hybrid UV photodetector with fast transient response and high responsivity was then fabricated from the ZnO QDs-Graphene composite material and organic polymers. The fast transient response and high responsivity of the device was attributed to high carrier transport and collection efficiency, together with ultrahigh active surface to volume ratio of the ZnO QDs-Graphene composite material. The published results from this study are also given in the Appendix.

4.4.4 ZnO ALD Quantum Dots for Li Ion Batteries

We also employed the ZnO ALD quantum dots for Li ion batteries. Zinc oxide is an inexpensive anode material. However, ZnO ALD has attracted less attention than other metal oxides due to its poor cycling stability. A rational design of ZnO nanostructures to control their particle sizes and microstructures is essential in order to improve their stability and performance as electrodes for lithium ion batteries. In this study, we grew ZnO quantum dots on graphene layers in the size regime from 2 to 7 nm. A relationship between size and electrochemical performance was observed, in which smaller sized QDs on graphene display enhanced electrochemical performance. A highly reversible specific capacity of 960 mAh g^{-1} was achieved at a current density of 100 mA g^{-1} for 2 nm ZnO QDs. This specific capacity is close to the theoretical value of ZnO as an anode for Li ion batteries. The results from this study are currently in press and are given in the Appendix.

4.4.5 SnO_2 ALD on Graphene for Li Ion Batteries

We have also synthesized SnO_2 ALD on graphene to form SnO_2 anodes for Li ion batteries. We found that SnO_2 ALD on graphene was an effective anode material. The SnO_2-Graphene composite exhibited a stable capacity of 800 mAh g^{-1} at 100 mA g^{-1} and 450 mAh g^{-1} at 1000 mA g^{-1}. Long cycling test at charge/discharge rates of 1A g^{-1} showed a very stable capacity and nearly 100% Coulombic efficiency. We are still finishing this study and will be writing a paper on these results very shortly.

5.0 CONCLUSIONS

In this work, we experimentally evaluated the impact of NO_2/TMA pretreatment on the nucleation and growth of ALD Al_2O_3 on a model sp^2 carbon substrate made from exfoliated HOPG. The ALD films on HOPG samples were evaluated using spectroscopic ellipsometry and electrochemical analysis to determine film thickness and quality. We found that 5 cycles of NO_2/TMA at 150°C deposits a ~8Å thick nucleation layer on HOPG, but produces no nucleation layer on the native oxide of silicon. The NO_2/TMA pretreatment enabled high quality, conformal, continuous ALD films after as few as 20 ALD cycles of TMA/H_2O. With no NO_2/TMA pretreatment, 100 ALD cycles of TMA/H_2O were necessary to produce a continuous film. Without pretreatment, thin Al_2O_3 ALD films (20 and 50 ALD cycles) were found to decrease charge transfer resistance at the electrode surface. Furthermore, a ~250Å Al_2O_3 film grown using 200 cycles of ALD Al_2O_3 without any pretreatment was found to have a higher initial through-film porosity and to degrade faster than a ~90 Å Al_2O_3 film grown using 50 cycles of Al_2O_3 with 5 cycles of NO_2/TMA pretreatment.

Additional studies evaluated the application of metal oxide ALD films on graphene and carbon nanotubes as electrodes for Li ion batteries, pseudocapacitance supercapacitors and ultraviolet sensors. TiO_2 ALD, ZnO ALD and SnO_2 ALD were the metal oxide ALD films that were explored for these applications. Publications resulting from this work on TiO_2 and ZnO ALD are given in the Appendix. In addition, further studies on SnO_2 ALD on graphene were also performed and are in the process of being written for publication.

6.0 REFERENCES

1. Schwierz, F. Graphene transistors. *Nat. Nanotechnol.* **5,** 487–96 (2010).

2. Knez, M., Nielsch, K. & Niinistö, L. Synthesis and Surface Engineering of Complex Nanostructures by Atomic Layer Deposition. *Adv. Mater.* **19,** 3425–3438 (2007).

3. Williams, J. R., Dicarlo, L. & Marcus, C. M. Quantum Hall effect in a gate-controlled p-n junction of graphene. *Science* **317,** 638–41 (2007).

4. Hou, J., Shao, Y., Ellis, M. W., Moore, R. B. & Yi, B. Graphene-based electrochemical energy conversion and storage: fuel cells, supercapacitors and lithium ion batteries. *Phys. Chem. Chem. Phys.* 15384–15402 (2011). doi:10.1039/c1cp21915d

5. Paek, S., Yoo, E. & Honma, I. Enhanced Cyclic Performance and Lithium Storage Capacity of SnO_2 / Graphene Nanoporous Electrodes with. 2–5 (2009).

6. Wang, D. *et al.* Self-Assembled TiO_2 – Graphene Hybrid Insertion. **3,** 907–914 (2009).

7. Wang, H. *et al.* Mn_3O_4-graphene hybrid as a high-capacity anode material for lithium ion batteries. *J. Am. Chem. Soc.* **132,** 13978–80 (2010).

8. Wu, Z. *et al.* Graphene Anchored with Co_3O_4 Nanoparticles as Anode of Lithium Ion Capacity and Cyclic Performance. **4,** 3187–3194 (2010).

9. Boukhalfa, S., Evanoff, K. & Yushin, G. Atomic layer deposition of vanadium oxide on carbon nanotubes for high-power supercapacitor electrodes. *Energy Environ. Sci.* **5,** 6872 (2012).

10. Lee, S. W., Kim, J., Chen, S., Hammond, P. T. & Shao-Horn, Y. Carbon nanotube/manganese oxide ultrathin film electrodes for electrochemical capacitors. *ACS Nano* **4,** 3889–96 (2010).

11. Sun, X. *et al.* Atomic Layer Deposition of TiO_2 on Graphene for Supercapacitors. *J. Electrochem. Soc.* **159,** A364 (2012).

12. Marichy, C. & Pinna, N. Carbon-nanostructures coated/decorated by atomic layer deposition: Growth and applications. *Coord. Chem. Rev.* **257,** 3232–3253 (2013).

13. Wang, X., Tabakman, S. M. & Dai, H. Atomic layer deposition of metal oxides on pristine and functionalized graphene. *J. Am. Chem. Soc.* **130,** 8152–3 (2008).

14. George, S. M. Atomic layer deposition: an overview. *Chem. Rev.* **110,** 111–31 (2010).

15. Cavanagh, A. S., Wilson, C. a, Weimer, A. W. & George, S. M. Atomic layer deposition on gram quantities of multi-walled carbon nanotubes. *Nanotechnology* **20,** 255602 (2009).

16. Farmer, D. B. & Gordon, R. G. Atomic layer deposition on suspended single-walled carbon nanotubes via gas-phase noncovalent functionalization. *Nano Lett.* **6,** 699–703 (2006).

17. Sun, X. *et al.* Pseudocapacitance of Amorphous TiO_2 Thin Films Anchored to Graphene and Carbon Nanotubes Using Atomic Layer Deposition. (2013).

18. Tato, W. Electrochemical Determination of the Porosity of Single and Duplex PVD Coatings of Titanium and Titanium Nitride on Brass. *J. Electrochem. Soc.* **145,** 4173 (1998).

19. Ahn, S. ., Choi, Y. ., Kim, J. . & Han, J. . A study on corrosion resistance characteristics of PVD Cr-N coated steels by electrochemical method. *Surf. Coatings Technol.* **150,** 319–326 (2002).

20. Ahn, S. ., Lee, J. ., Kim, H. . & Kim, J. . A study on the quantitative determination of through-coating porosity in PVD-grown coatings. *Appl. Surf. Sci.* **233,** 105–114 (2004).

21. Ott, A. W. *et al.* Modification of Porous Alumina Membranes Using Al_2O_3 Atomic Layer Controlled Deposition. **4756,** 707–714 (1997).

22. Elam, J. W., Groner, M. D. & George, S. M. Viscous flow reactor with quartz crystal microbalance for thin film growth by atomic layer deposition. *Rev. Sci. Instrum.* **73,** 2981 (2002).

APPENDIX - Publications Resulting from this Research

A. Chunmei Ban, Ming Xie, Xiang Sun, Jonathan J. Travis, Gongkai Wang, Hongtao Sun, Anne C. Dillon, Jie Lian and Steven M. George, "Atomic Layer Deposition of Amorphous TiO_2 on an Al_2O_3 Adhesion Layer on Graphene as an Anode for Li Ion Batteries", *Nanotechnology* **24**, 424002 (2013).

B. Xiang Sun, Ming Xie, Jonathan J. Travis, Gongkai Wang, Hongtao Sun, Jie Lian and Steven M. George, "Pseudocapacitance of Amorphous TiO_2 Thin Films Anchored to Graphene and Carbon Nanotubes using Atomic Layer Deposition", *J. Phys. Chem. C.* **117**, 22497-22508 (2013).

C. Dali Shao, Xiang Sun, Ming Xie, Mingpeng Yu, Steven M. George, Jie Lian and Shayla Sawyer, "ZnO Quantum Dots-Graphene Composite for Efficient Ultraviolet Sensing", *Mater. Lett.* **112**, 165-168 (2013).

D. Xiang Sun, Changgong Zhou, Ming Xie, Hongtao Sun, Tao Hu, Fengyuan Lu, Spencer M. Scott, Steven M. George, Jie Lian, "ZnO Quantum Dots/Graphene Nanocomposites by Atomic Layer Deposition with High Lithium Storage Capacity", *J. Mater. Chem. A* (In Press).

LIST OF ABBREVIATIONS

ALD	Atomic Layer Deposition
CVD	Chemical Vapor Deposition
EIS	Electrical Impedance Spectroscopy
HOPG	Highly Ordered Pyrolytic Graphite
SE	Spectroscopic Ellipsometry
TMA	Trimethylaluminum
XRR	X-ray reflectivity

DISTRIBUTION LIST

DTIC/OCP
8725 John J. Kingman Rd, Suite 0944
Ft Belvoir, VA 22060-6218 1 cy

AFRL/RVIL
Kirtland AFB, NM 87117-5776 1 cy

Official Record Copy
AFRL/RDHP, Susan Heidger 1 cy

This page intentionally left blank.